Chemistry and Physics of Lipids xxx (xxxx) xxx–xxx

Contents lists available at ScienceDirect

Chemistry and Physics of Lipids

journal homepage: www.elsevier.com/locate/chemphyslip

IR spectroscopy analysis of pancreatic lipase-related protein 2 interaction with phospholipids: 2. Discriminative recognition of various micellar systems and characterization of PLRP2-DPPC-bile salt complexes

Eduardo Mateos-Diaz[a], Priscila Sutto-Ortiz[a,b], Moulay Sahaka[a], Deborah Byrne[c], Hélène Gaussier[a], Frédéric Carrière[a,*]

[a] Aix-Marseille Université, CNRS, UMR7282 Enzymologie Interfaciale et Physiologie de la Lipolyse, Marseille, France
[b] Biotecnología Industrial, Centro de Investigación y Asistencia en Tecnología y Diseño del Estado de Jalisco A.C. (CIATEJ), Zapopan, Jalisco, México
[c] Aix-Marseille Université, CNRS, FR3479 Institut de Microbiologie de la Méditerranée, Marseille, France

ARTICLE INFO

Keywords:
Enzyme
FTIR spectroscopy
Lipids
Lipid digestion
Lipolysis
Phospholipase

ABSTRACT

The interaction of pancreatic lipase-related protein 2 (PLRP2) with various micelles containing phospholipids was investigated using pHstat enzyme activity measurements, differential light scattering, size exclusion chromatography (SEC) and transmission IR spectroscopy. Various micelles of 1,2-dipalmitoyl-*sn*-glycero-3-phosphocholine (DPPC) and lysophosphatidylcholine were prepared with either bile salts (sodium taurodeoxycholate or glycodeoxycholate) or Triton X-100, which are substrate-dispersing agents commonly used for measuring phospholipase activities. PLRP2 displayed a high activity on all phospholipid-bile salt micelles, but was totally inactive on phospholipid-Triton X-100 micelles. These findings clearly differentiate PLRP2 from secreted pancreatic phospholipase A2 which is highly active on both types of micelles. Using an inactive variant of PLRP2, SEC experiments allowed identifying two populations of PLRP2-DPPC-bile salt complexes corresponding to a high molecular weight 1:1 PLRP2-micelle association and to a low molecular weight association of PLRP2 with few monomers of DPPC/bile salts. IR spectroscopy analysis showed how DPPC-bile salt micelles differ from DPPC-Triton X-100 micelles by a higher fluidity of acyl chains and higher hydration/H-bonding of the interfacial carbonyl region. The presence of bile salts allowed observing changes in the IR spectrum of DPPC upon addition of PLRP2 (higher rigidity of acyl chains, dehydration of the interfacial carbonyl region), while no change was observed with Triton X-100. The differences between these surfactants and their impact on substrate recognition by PLRP2 are discussed, as well as the mechanism by which high and low molecular weight PLRP2-DPPC-bile salt complexes may be involved in the overall process of DPPC hydrolysis.

1. Introduction

The substrate specificity of lipolytic enzymes is strongly dependent on the supramolecular organization of the lipid substrates present in membranes, monolayers, micelles, vesicles or oil-in-water emulsions. Various kinetic models have been proposed to describe the mode of action of these enzymes including lipases and phospholipases. Among them, the Verger-De Haas'model is the adaptation of the Michaelis-Menten-Henri kinetic model to a two-dimensional space representing the lipid-water interface, combined with a first step of reversible enzyme adsorption at this interface (Verger et al., 1973a). It has been established and used in connection with the development of (phospho) lipase assays based on lipid monomolecular films and surface tensiometry (Verger and De Haas, 1973). The "surface dilution model" of Deems-Eaton-Dennis is based on the use of mixed micelles (Deems et al., 1975) and it was further adapted to liposomal dispersions, with the definition of the "scooting" and "hopping" modes of enzyme action (Gelb et al., 1995; Jain and Berg, 1989; Jain et al., 1995). All these models include an initial step of enzyme association with a supramolecular structure made by the susbtrate itself (liposomes, oil drops) or in which the substrate is embedded. The surface dilution model was for instance established to describe the action of cobra venom

Abbreviations: DLS, dynamic light scattering; DPPC, 1,2-di-palmitoyl phosphatidylcholine; EggPC, egg yolk phosphatidylcholine; FTIR, fourier transform infrared spectroscopy; FWHM, full width at half maximum; GPLRP2, guinea pig pancreatic lipase-related protein 2; LUV, large unilamellar vesicles; lyso-C16-PC, 1-palmitoyl-2-hydroxy-*sn*-glycero-3-phosphocholine; NaGDC, sodium glycodeoxycholate; NaTDC, sodium taurodeoxycholate; PLRP2, pancreatic lipase-related protein 2; SEC, size exclusion chromatography; $sPLA_2$-IB, pancreatic phospholipase A2; TX100, Triton X-100

* Corresponding author at: CNRS, UMR7282 EIPL, 31 chemin Joseph Aiguier, 13402 Marseille cedex 20, France.
E-mail address: carriere@imm.cnrs.fr (F. Carrière).

https://doi.org/10.1016/j.chemphyslip.2017.11.012
Received 6 September 2017; Received in revised form 14 November 2017; Accepted 15 November 2017

phospholipase A2 on mixed micelles made of 1,2-dipalmitoyl-sn-glycero-3-phosphorylcholine (DPPC) and Triton X-100, a non-ionic surfactant (Deems et al., 1975). Studies on pancreatic phospholipase A2 have often been carried out using surfactants naturally found in the small intestine, bile salts (De Haas et al., 1968).

Since pancreatic lipase-related proteins type 2 (PLRP2) is also present in pancreatic juice (De Caro et al., 1998) and displays a phospholipase A1 activity, mixed phospholipid-bile salts micelles have also been used to characterize the phospholipase activity of PLRP2. In a previous study, we have shown using IR spectroscopy that the guinea pig PLRP2 (GPLRP2) interacts preferentially with phospholipid molecules organized in mixed micelles with sodium taurodeoxycholate (NaTDC), which correlates with the enzyme activity on this substrate, but it shows no interaction with the same phospholipids organized in large unilamellar or multilamellar vesicles (Mateos-Diaz et al., 2017b). We extend here this study by the characterization of various phospholipid micelles and their interaction with GPLRP2 using dynamic light scattering (DLS) to analyze particle sizes, size-exclusion chromatography (SEC) to estimate the molecular weight and hydrodynamic diameter of protein-lipid-surfactant complexes, and infrared (IR) spectroscopy to study the effects of surfactants and GPLRP2 on the acyl chains, interfacial region and polar head-group of phospholipids. As previously described, we use an inactive variant (S152G) of GPLRP2 in order to study the enzyme binding to lipid aggregates with no interference of lipid hydrolysis.

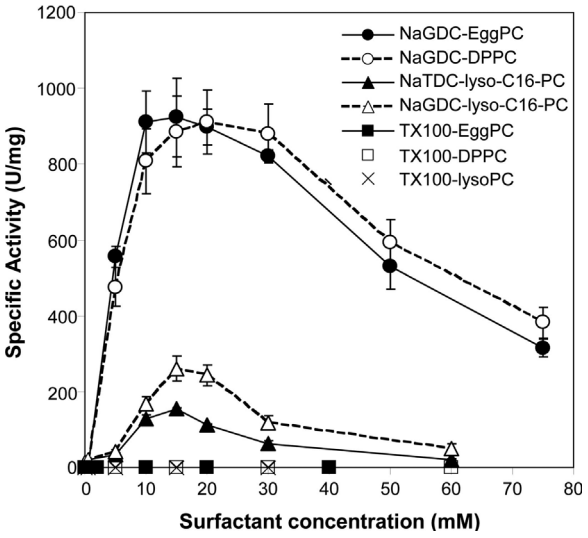

Fig. 1. Specific activity of GPLRP2 on egg yolk phosphatidylcholine (EggPC), 1,2-dipalmitoyl-sn-glycero-3-phospphocholine (DPPC) and 1-palmitoyl-2-hydroxy-sn-glycero-3-phosphocholine (lyso-C16-PC) as function of the surfactant concentration. Substrate concentrations were 17, 16 and 10 mM for EggPC, DPPC and lyso-C16-PC, respectively. Surfactant was either NaTDC, NaGDC or TX100. Initial reaction rates were obtained from pHstat titrimetric assays at 37 °C and pH 8.0. Values are means ± SD (n = 3).

2. Materials and methods

2.1. Reagents

1,2-dipalmitoyl-*sn*-glycero-3-phosphocholine (DPPC) and 1-palmitoyl-2-hydroxy-*sn*-glycero-3-phosphocholine (lyso-C16-PC) both > 99% purity were obtained from Echelon Biosciences Inc. Egg yolk phosphatidylcholine (EggPC) was obtained from Lipoid™. Sodium taurodeoxycholate (NaTDC), sodium glycoldeoxycholate (NaGDC), polyoxyethylene octyl phenyl ether or Triton X-100 (TX100), deuterium oxide (D_2O) 99.9%, benzamidine and dithiothreitol (DTT) were purchased from Sigma-Aldrich. Chloroform and methanol were from Carlo Erba. 2-(N-morpholino)-ethanesulfonic acid (MES), 2-Amino-2-(hydroxymethyl)propane-1,3-diol (Tris), 4-(2-hydroxyethyl)-1-piperazineethanesulfonic acid (HEPES), calcium chloride ($CaCl_2$) and sodium chloride (NaCl) were obtained from Euromedex.

2.2. Production and purification of wild-type GPLRP2 and S152G variant

Recombinant wild-type GPLRP2 (WT) was produced in *Aspergillus orizae* and purified as previously described (Hjorth et al., 1993). GPLRP2 S152G variant construction, production and purification from *Pichia pastoris* cultures are described in the accompanying article (Mateos-Diaz et al., 2017b). Stock solutions of GPLRP2 WT and S152G variant at 7.5 mg/mL (160 μM) were prepared in 100 mM MES buffer, 150 mM NaCl and 5 mM $CaCl_2$ at pH 6 for activity measurements, DLS and SEC, as well as in the same buffer in D_2O for IR experiments. A 10-fold dilution of these GPLRP2 stock solution (0.75 mg/mL, 16 μM) was used in all experiments.

2.3. Activity measurements of GPLRP2 on phospholipid-surfactant dispersions

Phospholipase and lysophospholipase activities of GPLRP2 were measured by automated titration of fatty acids released from stirred egg yolk phosphatidylcholine (EggPC), DPPC or lyso-C16-PC dispersions, using 0.1 N NaOH and a TTT80 Radiometer™ pHstat (Copenhagen). Each assay was performed in a thermostated (37 °C) vessel containing 1 mM buffer (Tris or MES for pH values around 8 and 6 respectively) with 150 mM NaCl and 5 mM $CaCl_2$. Routine assays were performed at pH 8 with a final substrate concentration of approximately 17, 16 and 10 mM for EggPC, DPPC and lyso-C16-PC respectively. One unit of enzymatic activity (U) corresponds to 1 μmol of free fatty acid released per min.

2.4. Preparation of phospholipid-surfactant micelles

DPPC-containing micelles for DLS and enzyme activity studies were prepared by dissolving first DPPC in chloroform:methanol 2:1 (v/v) and then evaporating the solvent under vacuum to obtain a thin film containing the necessary amount of lipid to get a final concentration of 5%, w/v (*i.e.* 68 mM DPPC). To form phospholipid micelles, the DPPC film was dissolved in 100 mM MES buffer, 150 mM NaCl and 5 mM $CaCl_2$ at pH 6 containing 50 mM of either NaTDC, NaGDC or TX100. The final phospholipid-to-surfactant molar ratio was 1.36, except when various amounts of surfactants were tested for their effects on enzyme activity (Fig. 1). The dispersions were then treated as previously described to yield mono dispersed mixed micelles at room temperature (Mateos-Diaz et al., 2017b). Similar procedures were used for preparing lyso-C16-PC micelles at a final concentration of 5% w/v (*i.e.* 100 mM), either with pure lyso-C16-PC or in the presence of NaTDC at a phospholipid-to-bile salt molar ratio of 0.5, except that no prior dissolution in chloroform-methanol was required because of the fast and efficient dissolution of lyso-C16-PC in MES buffer.

2.5. Dynamic light scattering measurements

Dynamic light scattering (DLS) experiments were carried out using a Zetasizer Nano S (Malvern Instruments) as previously described (Mateos-Diaz et al., 2017b). In some experiments, the temperature was increased by 5 °C-intervals from 25 to 70° to observe the thermotropic behavior of micellar dispersions (see Fig. S1). Three measurements were taken at each temperature, each one consisting in 10–15 runs of 10 s. The scattering angle was 173°. For each micellar dispersion, the determination of the hydrodynamic diameter (DH) was based on the Einstein-Strokes relation to obtain the intensity averaged size distribution. A viscosity of 0.8878 cP and a refractive index of 1.332 (at 25 °C) were used for the dispersion medium, while a value of 1.49 was used as an approximation of refractive index for micelles (Gagos et al., 2001). The changes in viscosity and refractive index induced by the

temperature were taken into account by the software algorithm. The data were analyzed with a customized method using 300 classes with a size-range analysis of 0.6 to 10000 nm.

2.6. Size exclusion chromatography (SEC) experiments

In order to investigate the formation of protein-lipid-surfactant aggregates upon GPLRP2 S152G interaction with DPPC and lyso-C16-PC micelles, SEC experiments were performed using a Prep Grade 16/60 SuperDex 75® column and an AKTA Explorer® fast protein liquid chromatography device. The column was equilibrated with 20 mM MES buffer (pH 6.0), 150 mM NaCl, 5 mM $CaCl_2$ at a flow rate of 1 mL/min. UV absorbance of the output flow was recorded continuously at 280 nm during column equilibration and elution of various samples: GPLRP2 S152G alone or in the presence of NaTDC, TX100, DPPC large unilamellar vesicle (LUV), or various micelles (DPPC-NaTDC, DPPC-NaGDC, DPPC-TX100, pure lyso-C16-PC, lyso-C16-PC-NaTDC). LUV were prepared as previously described (Mateos-Diaz et al., 2017b). The samples loaded onto the column (500 µL each) contained the same concentrations of phospholipids and surfactants as described in Section 2.4 and GPLRP2 S152G variant at a concentration of 16 µM (0.75 mg/mL). For each sample, the apparent molecular weight (Mw, Da) was estimated from the elution volume and the calibration of the column with ribonuclease A (13.7 kDa), chymotrypsinogen A (25 kDa), ovalbumine (43 kDa) and Albumine (67 kDa). Stokes radius (R_H, Å)/hydrodynamic diameter (D_H, nm) was estimated from the following equation according to Uversky (Uversky, 1993) and assuming that GPLRP2 S152G is a compact folded globular protein:

$$\log_{10}(R_H) = 0.369 \times \log_{10}(\mathrm{Mw}) - 0.254 \quad (1)$$

2.7. Infrared spectroscopy experiments

For IR studies, phospholipid-surfactant dispersions and stock solution of GPLRP2 S152G variant at 7.5 mg/mL (160 µM) were prepared in D_2O buffer as previously described (Mateos-Diaz et al., 2017b) to avoid the presence of water bands in the IR-spectra. The protein in D_2O buffer was added to the micelle solution at a final concentration of 0.75 mg/mL (16 µM), just before recording the transmission IR spectrum. All IR-spectra were recorded with a JASCO™ FT/IR-6100 Fourier transform infrared spectrometer, analyzed and deconvoluted as previously described (Mateos-Diaz et al., 2017b). The analysis of the temperature-induced changes of different spectral bands, especially CH_2 asymmetric stretching band, was performed by fitting the data with the *two state model* equation proposed by Kirchhoff (Kirchhoff and Levin, 1987; Mateos-Diaz et al., 2017b). It allowed estimating the main phase transition temperature (T_m; sigmoid midpoint) and $1/k$, a parameter proportionally related to phase transition cooperativity.

3. Results

3.1. Phospholipase activity of GPLRP2 on various phospholipid micelles

We measured the phospholipase activity of GPLRP2 on EggPC, DPPC and lyso-C16-PC in various micellar systems, using various concentrations of anionic bile salts (*i.e.* NaGDC and NaTDC) or non-ionic detergent Triton X-100 (Fig. 1). In the absence of surfactants, no hydrolytic activity was detected on diacylphospholipids (EggPC or DPPC) and only very low activity was measured with lyso-C16-PC (16 U/mg). In the presence of NaGDC, high phospholipase activities on both EggPC and DPPC were measured with maxima of 924 ± 104 and 911 ± 84 U/mg, respectively. These maximum activities were recorded in the 10 to 20 mM bile salt concentration range, which corresponds to a phospholipid-to-surfactant molar ratio between 0.8 and 1.7. Similarly, the addition of bile salts allowed measuring significant activities on lyso-C16-PC with maxima of 153 ± 5 and 261 ± 33 U/mg with NaTDC and NaGDC, respectively. These maximum activities were recorded in the 15 to 20 mM bile salt concentration range, which corresponds to a phospholipid-to-surfactant molar ratio between 0.5 and 0.7. No enzymatic activity was detected when TX100 was used as surfactant instead of bile salts, regardless of the substrate. However, some lipolytic activity could be measured when bile salts were added in the course of the assays with TX100-phospholipid dispersions (data not shown). It is worth noticing that GPLRP2 activity on PC-bile salt mixed micelles was still relatively important (≈50% of maximum) at the bile salt concentration of 50 mM that was further used in DLS, SEC and IR experiments (see the following sections).

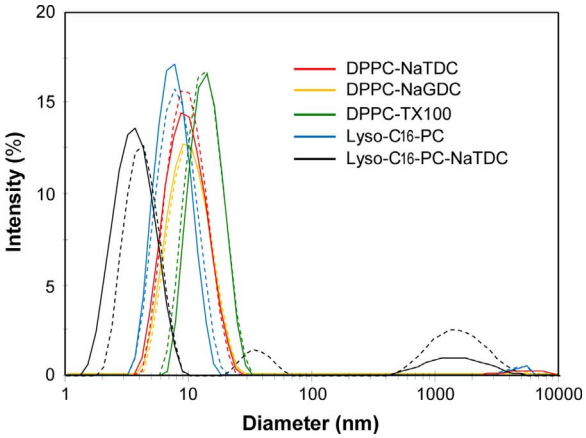

Fig. 2. Size distribution of various micellar systems based on the intensity of dynamic light scattering (DLS). Diacylphospholipid, lyso-C16-PC and surfactant (NaTDC, NaGDC or TX100) concentrations were 68 mM, 100 mM and 50 mM, respectively, to ensure phospholipid-to-surfactant molar ratio of 1.36 with diacylphospholipids and 0.5 with lysophospholipids. Dispersions containing the GPLRP2 S152G variant are shown as dashed lines. All experiments were performed at pH 6 and 35 °C.

3.2. Particle size analysis by DLS of the various micelle systems

The particle size distribution of aggregates present in the phospholipid-surfactant dispersions was determined by dynamic light scattering at 35 °C and pH 6 (Fig. 2). DLS experiments confirmed that all the tested dispersions contained predominantly micelles. On average, DPPC-bile salt mixed micelles displayed a hydrodynamic diameter of about 9 to 10 nm, while DPPC-TX100 mixed micelles were slightly bigger with an average diameter of about 12 nm (Table 1). Lyso-C16-PC-containing dispersions were slightly smaller with an average

Table 1
Hydrodynamic diameter (D_h, z-average) and polydispersity index (PdI) of various micellar systems. D_h and PdI were determined for the micelles alone and in the presence of the inactive GPLRP2 S152G variant (0.75 mg/mL or). Dispersions contained either 5% of DPPC (68 mM) or lyso-C16-PC (100 mM), with lipid-to-surfactant molar ratio of 1.36 and 0.5, respectively. All experiments were performed at pH 6 and 35 °C. Values are means ± SD of at least 3 independent assays.

Micelles	Dh (nm)	PdI
DPPC-NaTDC	9.1 ± 0.5	0.164
DPPC-NaTDC + GPLRP2 S152G	8.6 ± 0.2	0.122
DPPC-NaGDC	9.4 ± 0.4	0.165
DPPC-NaGDC + GPLRP2 S152G	9.7 ± 0.7	0.182
DPPC-TX100	12.3 ± 0.2	0.089
DPPC-TX100 + GPLRP2 S152G	12.3 ± 0.2	0.097
lyso-C16-PC	7.2 ± 0.2	0.185
lyso-C16-PC + GPLRP2 S152G	7.1 ± 0.1	0.132
Lyso-C16-PC-NaTDC	3.4 ± 0.1	0.185
Lyso-C16-PC-NaTDC + GPLRP2 S152G (z-average value of a mixture of 3 populations centered at 4, 35 and 1500 nm)	64.6 ± 2.2	0.293

diameter of about 7 nm for pure lyso-C16-PC and around 3 nm for lyso-C16-PC-NaTDC mixed micelles. The average hydrodynamic diameter of lyso-C16-PC containing micelles remained unchanged upon increasing the temperature while that of DPPC-bile salt and DPPC-TX100 mixed micelles drastically increased above 35 °C (Fig. S1A). This was mainly due to an increased heterogeneity in particle size distribution and an increased proportion of large aggregates (Fig. S1B). The hydrodynamic diameter (Table 1) and the size distribution (Fig. 2) of micelles were not significantly changed upon addition of the GPLRP2 S152G variant, except for the lyso-C16-PC-NaTDC system, for which two additional size populations of higher diameter (≃35 and 1500 nm) could be detected. Increasing the temperature had also a drastic impact on this latter system in the presence of GPLRP2 S152G variant, with a strong increase in the average hydrodynamic diameter that reached values above the detection limit of the DLS technique (Fig. S1A).

3.3. Size exclusion chromatography (SEC) experiments

In addition to DLS analysis, SEC experiments were performed with GPLRP2 S152G variant alone and in the presence of surfactants (NaGDC, NaTDC or TX100), DPPC LUV or mixed micelles (DPPC-NaTDC, DPPC-NaGDC, DPPC-TX100, pure lyso-C16-PC and lyso-C16-PC-NaTDC). Pure GPLRP2 S152G variant was eluted from the Prep Grade 16/60 SuperDex 75® column using approximately 54 mL of elution buffer, which was also the case for GPLRP2 S152G variant incubated with LUV as judged from UV absorbance at 280 nm (Fig. 3). With LUV, a strong absorbance was also observed at lower elution volume (around 40 mL) which is due to UV light diffraction by liposomes having a similar size to the wavelength of UV light. In the presence of DPPC-NaTDC and DPPC-NaGDC mixed micelles, the protein elution occurred earlier with a main peak corresponding to a volume of 52 mL, suggesting the formation of GPLRP2-DPPC-bile salt complexes. In both cases, a smaller peak was also observed after an elution volume of 40 mL for DPPC-NaTDC micelles and 41 mL for DPPCNaGDC micelles, which might correspond to high Mw enzyme-micelle complexes. From the AUC ratio of the two peaks of UV absorbance centered at 40 and 52 mL (Fig. 3), we could estimate that around 10% of GPLRP2 S152 variant is present in high Mw enzyme-DPPC-NaTDC complexes while 90% is present in low Mw enzyme-DPPC-NaTDC complexes. Similar values were obtained with NaGDC-DPPC micelles.

When GPLRP2 S152G variant was incubated with the surfactants alone or lyso-C16-PC, the protein elution occurred slightly later using a volume of 55 to 56 mL, which might reflect slight changes in the protein shape induced by the surfactants. A smaller peak was however observed at an elution volume of 40 mL when GPLRP2 S152G was mixed with Triton X100, which might correspond to some high Mw GPLRP2-TX100 complexes. These aggregates were not observed when GPLRP2 S152G was mixed with both TX100 and DPPC.

Based on the calibration of the SEC column with proteins of various molecular weights (Mw), we estimated an apparent Mw of 47,566 Da for GPLRP2 S152G alone, that was close to the Mw of GPLRP2 S152G molecular weight deduced from its amino acid sequence (47,647 Da; no glycosylation), and a hydrodynamic diameter of 5.9 nm fitting with the known protein dimensions (Withers-Martinez et al., 1996). Similar values were obtained with the other systems (Table 2), except with DPPC-NaTDC and DPPC-NaGDC mixed micelles, for which the apparent Mw increased significantly and displayed two populations. The main one contained around 90% of the protein as judged from the UV absorbance and was characterized by an increase in Mw of 8.5% with NaGDC (51,678 Da) and 10.4% with NaTDC (52,611 Da) and an estimated hydrodynamic diameter of 6.2 nm (+3.8% compared to GPLRP2 S152G alone; Table 2) with both bile salts. The second and minor population (10% of the protein) was characterized by a much higher increase in Mw of 123.3% with NaGDC (106,419 Da) and 134.8% with NaTDC (111,887 Da) and estimated hydrodynamic diameters of 8.0 and 8.1 nm, respectively (+35 and 37% compared to GPLRP2 S152G alone; Table 2).

Interestingly, when GPLRP2 S152 G was mixed with surfactants alone (NaTDC, TX100), lyso-C16-PC with or without NaTDC and DPPC-TX100 mixed micelles, the apparent Mw deduced from SEC was lower than the molecular weight of the protein alone (Table 2). These changes in the hydrodynamic properties of GPLRP2 S152 maybe due to the interaction of surfactants with the protein and some conformational changes as often observed with lipases (Mateos-Diaz et al., 2017a). These changes can impact on the protein shape and compactness.

3.4. Infrared spectroscopy analysis of DPPC and lyso-C16-PC micellar systems

Transmission IR spectra of DPPC and lyso-C16-PC dispersions in D_2O and at pD 6 were recorded and C—H stretching vibrations were analyzed to get information on the fluidity of the hydrophobic acyl chains. Differences in vibration frequency (wavenumber) and full width at half maximum (FWHM) values were observed (Fig. 4 and Table 3). For instance, DPPC LUV presented the lowest wavenumber and FWHM values, followed by DPPC-TX100, DPPC-bile salts and lyso-C16-PC micelles. The addition of GPLRP2 S152G variant altered neither the frequency nor the FWHM value of LUV and DPPC-TX100 micelles. It increased however the FWHM value of lyso-C16-PC-containing dispersions, while it reduced FWHM and frequency values of DPPC-bile salt systems.

Both the wavenumber and FWHM values of $_{as}(CH_2)$ of DPPC dispersions showed a typical sigmoidal increase upon increasing the temperature, while the $\nu_{as}(CH_2)$ of lyso-C16-PC evolved rather linearly

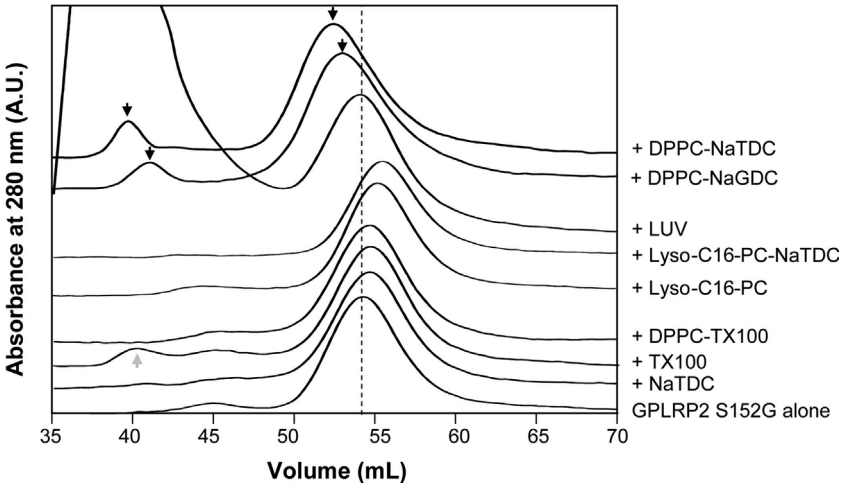

Fig. 3. Size exclusion chromatography (SEC) elution profile of GPLRP2 S152G variant in the presence of various phospholipid-surfactant dispersions. Dispersions contained either 5% of DPPC (68 mM) or lyso-C16-PC (100 mM), with lipid-to-surfactant molar ratio of 1.36 and 0.5, respectively. In controls surfactants were tested at 50 mM. Small black and grey arrows indicate the most relevant changes in GPLRP2 S152 elution in the presence of DPPC-bile salt micelles and Triton X-100, respectively. All the experiments were performed at pH 6 at least in duplicate and only representative elution profiles are shown here.

Table 2
Theoretical molecular weight (Mw) and hydrodynamic diameter (D_H) of GPLRP2 S152G variant estimated from size exclusion chromatography (SEC) in the presence of various phospholipid-containing dispersions. All experiments were performed at pH 6. Values are means ± SD of at least 3 independent assays.

Sample	*Apparent Mw* (Da)	*ΔMw vs. GPLRP2 Mw* (Da)	CV%	R_H (Å)	D_H (nm)	ΔD_H (nm)	CV%
GPLRP2 S152G alone	47,566	−81	−0.2	29.6	5.9	0.00	0.0
GPLRP2 S152G + LUV	47,058	−589	−1.2	29.5	5.9	−0.02	−0.4
GPLRP2 S152G + NaTDC	46,168	−1478	−3.1	29.3	5.9	−0.06	−1.1
GPLRP2 S152G + TX100	45,894	−1753	−3.7	29.2	5.8	−0.08	−1.3
GPLRP2 S152G + DPPC-NaTDC (main peak)	52,611	4964	+10.4	30.8	6.1	+0.22	+3.8
GPLRP2 S152G + DPPC-NaTDC (small peak)	111,887	64,240	+134.8	40.6	8.1	+2.20	+37.1
GPLRP2 S152G + DPPC-NaGDC (main peak)	51,678	4031	+8.5	30.8	6.1	+0.22	+3.8
GPLRP2 S152G + DPPC-NaGDC (small peak)	106,419	58,772	+123.3	39.9	8.0	+2.05	+34.6
GPLRP2 S152G + DPPC-TX100	46,086	−1561	−3.3	29.3	5.9	−0.07	−1.2
GPLRP2 S152G + lyso-C16-PC	44,839	−2808	−5.9	29.0	5.8	−0.13	−2.2
GPLRP2 S152G + lyso-C16-PC-NaTDC	44,599	−3048	−6.4	28.9	5.8	−0.14	−2.3

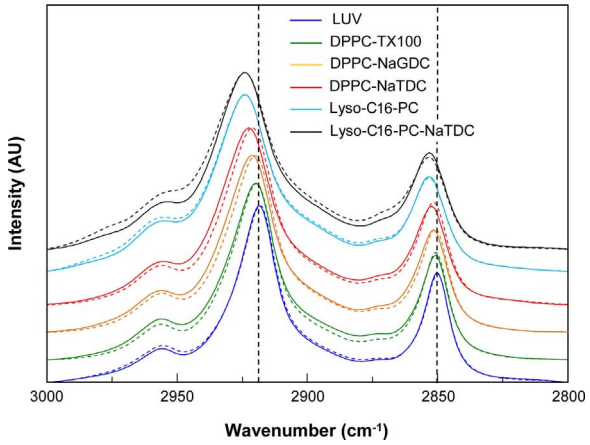

Fig. 4. CH stretching vibrations of various DPPC and lyso-C16-PC dispersions in the presence and absence of surfactant. Solid lines represent the spectra of dispersions alone and dashed lines those recorded in the presence of GPLRP2 S152G variant. NaGDC, NaTDC and TX100 were used as surfactants. All experiments were performed at 35 °C and pD 6.

(Fig. S2). The main phase transition temperature (T_m) and cooperativity parameter (1/k) for DPPC dispersions were obtained by fitting the data with Kirchhoff's two state model equation (Fig. 5 and Table S1). DPPC-TX100 mixed micelles and DPPC LUV displayed the highest 1/k and T_m values, while DPPC-bile salt mixed micelles displayed the lowest ones. No T_m and cooperativity values could be estimated for lyso-C16-PC-containing systems. However, it worth mentioning that the overall vibration frequencies of the $\nu\nu_{as}(CH_2)$ of lyso-C16-PC systems were higher than those of DPPC preparations (Fig. S2). The addition of GPLRP2 S152G variant had no major effects on the thermotropic parameters of DPPC-TX100 dispersion, as also observed with DPPC LUV, while it induced an increase of the T_m of both DPPC-bile salt mixed micelles, particularly with NaTDC and to a lesser extent with NaGDC (Fig. 5). Significant and opposite changes in the cooperativity values were also observed with DPPC-NaTDC and DPPC—NaGDC mixed micelles. No changes in $\nu_{as}(CH_2)$ frequency were observed upon mixing GPLRP2 S152G variant with the lyso-C16-PC-containing systems, but an increase in FWHM values was however observed for both dispersions (Table 3).

The carbonyl (CO) stretching region of the IR spectra was also analyzed after deconvolution (Fig. 6 and Table 3). The line-shape of CO stretching spectrum of DPPC in the presence of NaGDC (Fig. 6A) was very close to that previously observed with NaTDC (Mateos-Diaz et al., 2017b), while, interestingly, in the presence of TX100 (Fig. 6B) it was closer to that observed with LUV (Mateos-Diaz et al., 2017b). The main difference between NaGDC and TX100-containing systems was the relative intensity of the two subcomponents at around 1740 cm^{-1} (non-H-bonded) and 1730 cm^{-1} (H-bonded) arising after deconvolution. The CO stretching spectrum of DPPC-TX100 mixed micelles displayed a more prominent high frequency subcomponent (1740 cm^{-1}), while the lower frequency subcomponent (1730 cm^{-1}) was more prominent with DPPC-NaGDC mixed micelles. The thermotropic analysis of the 1730/1740 cm^{-1} intensity ratio for DPPC-NaGDC mixed micelles (Fig. S3A) showed a very similar profile to that observed for the DPPC-NaTDC micelles (Mateos-Diaz et al., 2017b). Moreover, in both cases the addition of GPLRP2 S152G variant decreased the 1730/1740 cm^{-1} intensity ratio at temperatures below 40 °C (Figs. 6 A, Fig. S3A and (Mateos-Diaz et al., 2017b)). Interestingly, these effects were not observed with DPPC-TX100 mixed micelles (Fig. 6B and Fig. S3A), which actually presented the lowest values of the CO subcomponents intensity ratio of all systems studied, including LUV.

In contrast to DPPC dispersions, lyso-C16-PC dispersions presented three CO-band subcomponents at 1740, 1725 and 1710cm^{-1} (Fig. 6C and D), with the one at 1725 cm^{-1} being the most intense and resulting in an overall lower vibration frequency of the raw CO spectrum compared to DPPC containing systems (Fig. 6A and B). The presence of NaTDC (Fig. 6D) induced a change in the line-shape of the spectra, apparently related to a decreased in the width of some of the

Table 3
Summary of the relevant IR spectral parameters of different phospholipid dispersions in the absence and presence of GPLRP2 S152G variant. All the experiments were performed at 35 °C and pD 6. Values are means ± SD of at least 3 independent assays.

Lipid system	Alone				+ S152G variant (difference)			
	νas(CH2)		ν(CO)	Head-group	νas(CH2)		ν(CO)	Head-group
	Wavenumber (cm^{-1})	FWHM (cm^{-1})	Intensity ratio	FWHM (cm^{-1})	Wavenumber (cm^{-1})	FWHM (cm^{-1})	Intensity ratio	FWHM (cm^{-1})
LUV	2918.7 ± 0.1	19.91 ± 0.02	0.866 ± 0.002	60.40 ± 0.50	0.0 ± 0.1	0.00 ± 0.02	0.00 ± 0.003	0.26 ± 0.25
DPPC-NaTDC	2923.2 ± 0.1	24.91 ± 0.35	1.097 ± 0.014	51.98 ± 0.22	−0.9 ± 0.1	−0.47 ± 0.00	−0.05 ± 0.024	−2.98 ± 0.10
DPPC-NaGDC	2922.7 ± 0.2	24.94 ± 0.09	1.092 ± 0.016	55.65 ± 0.44	−0.7 ± 0.2	−0.64 ± 0.57	−0.08 ± 0.022	−4.61 ± 0.26
DPPC-TX100	2920.8 ± 0.2	23.54 ± 0.53	0.846 ± 0.004	51.96 ± 0.11	−0.2 ± 0.2	−0.93 ± 0.53	−0.01 ± 0.009	−0.24 ± 1.27
Lyso-C16-PC	2923.9 ± 0.1	26.72 ± 0.06	1.995 ± 0.066	45.45 ± 0.43	0.1 ± 0.1	0.77 ± 0.14	0.05 ± 0.062	1.87 ± 0.22
Lyso-C16-PC-NaTDC	2924.0 ± 0.1	26.17 ± 0.17	2.262 ± 0.000	44.59 ± 0.68	0.1 ± 0.1	2.25 ± 0.13	−0.02 ± 0.093	4.40 ± 0.54

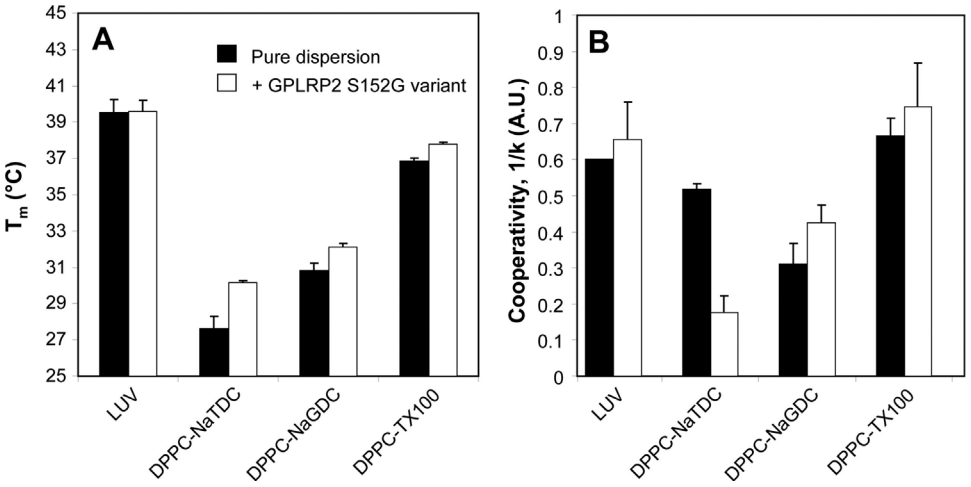

Fig. 5. Relevant thermotropic parameters for the CH2 asymmetric stretching band shift recorded with various phospholipid dispersions. DPPC was at 5% (w/v) in liposomes, DPPC-NaTDC, DPPC-NaGDC, DPPC-TX100 (1.36:1.00 molar ratio) mixed micelles, as well as lyso-C16-PC in simple micelles and lyso-C16-PC-NaTDC (1:2 molar ratio) mixed micelles, alone or in presence of GPLRP2 S152G variant at pD 6.

subcomponents, but, in general, it did not affect their vibration frequencies and/or relative intensities. The 1740/1725 cm^{-1} intensity ratio was only slightly decreased upon increasing the temperature and this variation was rather linear (Fig. S3B). Moreover, it presented much higher values between 2 and 2.3 compared to the intensity ratio estimated for the DPPC-containing systems (Fig. S3A and Table 3). The addition of GPLRP2 S152G variant slightly affected the line-shape but not the relative intensities of the CO stretching band subcomponents (Table 3).

The region of the IR spectra between 1130 and 1030 cm^{-1} containing the symmetric PO and R—O—P—O—R' stretching bands was also analyzed (Fig. 7). The spectral line-shape of DPPC containing dispersions was similar (Figs. 7A and B), except for a shoulder at 1052 cm^{-1}, which appeared more intense with DPPC—NaGDC mixed micelles. Upon addition of GPLRP2 S152G variant, the bands subcomponents at 1088 and 1069 cm^{-1} remained practically unchanged for both systems, but the vibration band at 1052 cm^{-1} significantly decreased in the case of DPPC-NaGDC mixed micelles (Figs. 7A). In the case of lyso-C16-PC dispersions (Figs. 7C and D), the line-shape was slightly different and the vibration frequencies were lower than those observed with DPPC dispersions. The presence of NaTDC (Figure D) did not affect the shape of the lyso-C16-PC spectrum in this region. However, upon addition of GPLRP2 S152G variant, the apparition of a band at 1050 cm^{-1} was only observed in the case of lyso-C16-PC-NaTDC mixed micelles (Fig. 7D), which is exactly opposed to what we observed with DPPC-bile salt mixed micelles (Fig. 7A).

4. Discussion

4.1. GPLRP2 hydrolyses DPPC present in mixed micelles containing bile salts but not in those containing non-ionic triton X-100

The effects of surfactant molecules on the activity of lipolytic enzymes have long been recognized. Their amphiphilic properties allow them to interact with both the enzyme (Mateos-Diaz et al., 2017a, 2007) and the lipids (Helenius and Simons, 1975; Schurtenberger et al., 1985), changing their interfacial properties and resulting in complex kinetic behaviors (Berg et al., 2001, 1991; Deems et al., 1975; Panaitov et al., 1997; Verger et al., 1973b). The secreted pancreatic phospholipase A2 (sPLA2-IB) shows for instance a much higher activity on phosphatidylcholine present in mixed micelles with surfactants than on monolayers at low surface pressure, and is not active on membranes (Verger et al., 1973b). sPLA2-IB presents an "interfacial activation" in the presence of phospholipid micelles (de Haas et al., 1971) and is active on mixed micelles made with both bile salts (De Haas et al., 1968) and Triton X-100 (Deems et al., 1975; Dennis, 1973). Similarly, we have shown previously that GPLRP2 displays a high phospholipase A1 activity when the PC substrate is in the form of mixed micelles with deoxycholate (Hjorth et al., 1993) or NaTDC (Mateos-Diaz et al., 2017b), a lower activity on PC monolayers and only at low surface pressure (Hjorth et al., 1993), and no activity on PC large uni- or multilamellar vesicles (Mateos-Diaz et al., 2017b). Here we show that these findings can also be extended to another bile salt like NaGDC, but

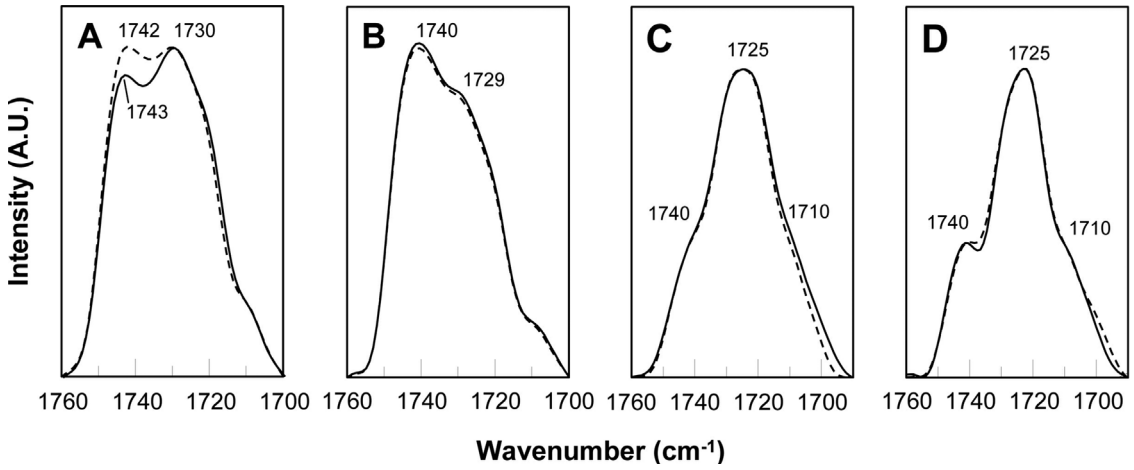

Fig. 6. Deconvolved IR-spectra of CO stretching vibration of various phospholipid-surfactant dispersions. DPPC-NaGDC (A), DPPC-TX100 (B), pure lyso-C16-PC (C) and lyso-C16-PC-NaTDC (D) systems at 35 °C and pD 6 are shown from right to left. Solid lines represent dispersions alone and dashed lines dispersions in the presence of GPLRP2 S152G variant. The DPPC-surfactant molar ratio was 1.36:1.00 and lyso-C16-PC-NaTDC molar ratio was 1:2.

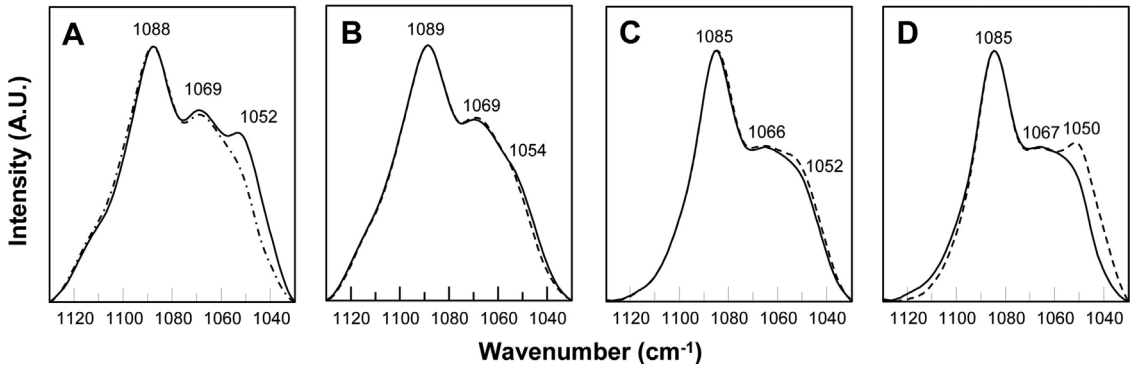

Fig. 7. IR spectrum of the head-group vibrations in the region between 1130 and 1030 cm^{-1} of DPPC-NaGDC (A), DPPC-TX100 (B), pure lyso-C16-PC (C) and lyso-C16-PC-NaTDC (D) systems, alone (solid line) and in the presence of GPLRP2 S152G variant (dashed line). The experiments were performed at 5% (w/v) of DPPC or lyso-C16-PC in D_2O at pD6 and at a S152G variant concentration of 0.75 mg/mL. The lipid-to-surfactant (NaGDC, NaTDC or TX100) molar ratio was 1.36 or 0.5 in DPPC and lyso-C16-PC systems respectively.

GPLRP2 appears to be totally inactive on various TX100-phospholipid micelles prepared with EggPC, DPPC or lyso-C16-PC (Fig. 1). This is a striking difference between GPLRP2 and sPLA2-IB, and GPLRP2 therefore appears to be a more discriminative enzyme with respect to its interaction with mixed surfactant-phospholipid micelles. Interestingly, the absence of GPLRP2 activity on mixed TX100-DPPC micelles could be reversed by the addition of NaTDC during the activity assay, suggesting that TX100 molecules impair the interaction of GPLRP2 with lipid-water interface and are displaced by NaTDC molecules. Another explanation for the absence of GPLRP2 activity in the presence of TX100 could also be the binding of TX100 within the enzyme active site, as observed by X-ray crystallography with other pancreatic lipases and surfactants (Hermoso et al., 1996; Mateos-Diaz et al., 2017a) but this type of interaction has never been shown to be deleterious for enzyme activity. The discrimination between mixed micelles by GPLRP2 seems therefore to result from distinct interfacial properties of the lipid aggregates. While it is inactive in the presence of TX100, GPLRP2 retains its catalytic activity at very high bile salt concentrations (> 70 mM; Fig. 1). Besides their essential role in the solubilization of the phospholipid substrate and lipolysis products, these surfactants appear to be critical for the interaction of GPLRP2 with its phospholipid substrate. PLRP2 could thus be viewed as a bile salt-dependent phospholipase like the so-called bile salt-stimulated lipase (Hernell and Olivecrona, 1974). Similar features were observed with both the initial phospholipid substrate and lysophospholipids which are intermediary lipolysis products. Conversely, both phospholipids and lysophospholipids were not hydrolyzed by PLRP2 in the presence of TX100. This non-ionic surfactant and bile salts have therefore distinct effects on the solubilization of both substrate (phospholipids) and lipolysis products (lysophospholipids).

4.2. Size exclusion chromatography reveals the formation of two populations of GPLRP2-DPPC-bile salts complexes

The exact physical structure of phospholipid-bile salt mixed micelles is still a matter of debate (Kozlov et al., 1997). Several models have been proposed based on X-ray diffraction, NMR, DLS studies and molecular dynamic simulations, describing micelles with disk-shaped, rod-like and/or worm-like geometries (Cohen et al., 1998; Hjelm et al., 1992; Madenci et al., 2011; Mazer et al., 1980; Nichols and Ozarowski, 1990; Walter et al., 1991). Other studies suggest that all these different molecular organizations may actually exist in equilibrium under certain specific conditions and other might just be kinetic entrapped structures or intermediaries (Egelhaaf and Schurtenberger, 1999). The exact structure of phospholipid-TX100 mixed micelles is also a matter of debate. They seem to be organized as thread-like structures under certain conditions and/or as rods/ellipsoids under others (Almgren, 2000). For simplicity and for further discussion, DPPC mixed micelles with bile salt are depicted here as the cross-section of a disk/cylinder with bile salt molecules accumulating at the edges, but also present at the middle DPPC-rich regions, either as oligomers interacting with other bile salt and DPPC molecules or as monomers embedded in the interface and interacting only with DPPC molecules (Fig. 8).

SEC experiments allowed observing the interaction of GPRLP2 S152G variant with mixed DPPC-bile salts micelles (Fig. 3) and two populations of protein-containing aggregates were identified. In the larger one (90% of the protein), the apparent molecular weight deduced from the SEC experiments (51–52 kDa; + 9-10% with respect to the protein alone) might correspond to GPLRP2 in complex with a few molecules of DPPC and/or bile salts (Fig. 8). In the second and minor population (10%), the apparent molecular weight value (106–112 kDa; + 123-135% with respect to the protein alone) and the hydrodynamic diameter (around 8 nm versus 5.9 nm for the protein alone) are consistent with large GPLRP2-micelle complexes made of one enzyme molecule and one mixed DPPC-bile salt micelle (Fig. 8). Based on the increase in the apparent molecular weights versus GPLRP2 S152 alone (Table 2) and the DPPC to bile salt molar ratio of 1.36, we could estimate that GPLRP2 S152 might interact with mixed micelles made of either 57 DPPC and 42 NaTDC molecules or 54 DPPC and 40 NaGDC molecules. These values are consistent with those reported in the literature for disk-shape or rod-like mixed micelles of phospholipid and bile salts micelles (Dennis, 1974; Nichols and Ozarowski, 1990).

While SEC is specific of GPLRP2-bound particles and allows observing GPLRP2 interaction with phospholipids-bile salts micelles, DLS does not reveal significant changes in the average particle size and distribution when the protein is mixed with these micelles (Table 1 and Fig. 2). Since rather broad size distributions are observed and DLS gives only an average hydrodynamic radius assuming spherical aggregates, one cannot exclude that complexes are formed. DLS data probably reflect the main population of micelles which is that of free micelles. Indeed we used a large excess of micelles versus GPLRP2 molecules, which is estimated to be close to 75–80 based on the estimated micelle composition. DLS gives a slightly higher hydrodynamic diameter for DPPC-bile salt micelles (around 9 nm) compared to the hydrodynamic diameter estimated by SEC for GPLRP2-micelle complexes (around 8 nm). Nevertheless, if we take into account that these size estimations are based on different physical properties and calculations, both SEC and DLS experiments allow determining particle sizes in the same range when GPLRP2 and DPPC-bile salt micelles are mixed, at least for one subpopulation of GPLRP2-DPPC-bile salt complexes.

SEC experiments revealed that the fraction of GPLRP2 S152G variant present in the high Mw subpopulation of enzyme-DPPC-bile salt complexes is lower (10%) than the fraction associated with the low Mw subpopulation (90%). This suggests that high Mw enzyme-micelle complexes are transiently formed upon the interaction of GPLRP2 S152G variant and further dissociate, giving rise to low Mw enzyme-

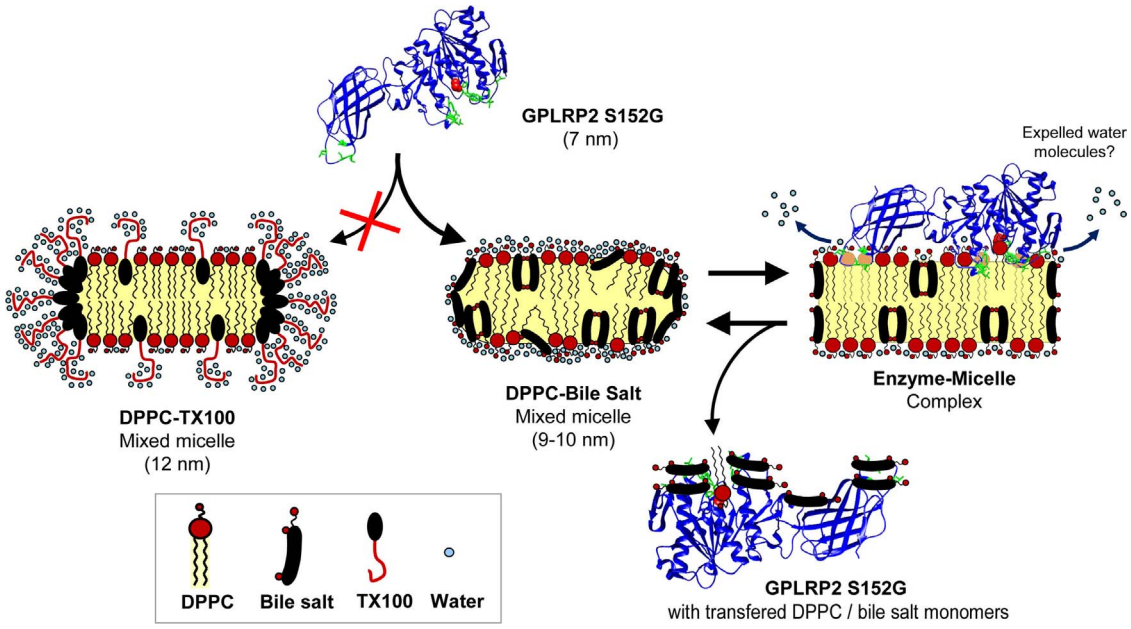

Fig. 8. Schematic representation of DPPC-Triton X100 mixed micelles, DPPC-NaTDC mixed micelles and GPLRP2 S152G interaction with DPPC-NaTDC micelles and individual molecules. The 3D model of GPLRP2 S152G variant is shown as a ribbon Cα-tracing (blue color) based on the X-ray structure of the GPLRP2-HPL chimera (Withers-Martinez et al., 1996). The active site serine residue is indicated by red spheres. The hydropobic residues present in GPLRP2 lipid binding site are shown as sticks and are colored in green. The disk-shape structure of DPPC-NaTDC micelles is based on Mazer's model (Mazer et al., 1980). The number of DPPC and NaTDC monomers (4 of each) bound to GPLRP2 after the interaction with micelles is based on the molecular weight increased deduced from SEC experiments. (For interpretation of the references to colour in this figure legend, the reader is referred to the web version of this article.)

DPPC-bile salt complexes, in which only a few molecules of DPPC and/or bile salt are transferred from the mixed micelles to the protein. Several combinations of DPPC and bile salt molecules can be used to fit with the increase in the apparent Mw of GPLRP2 S152G variant, ranging from 6 to 7 molecules of DPPC alone to 8 to 11 molecules of bile salt alone, depending of DPPC-bile salt system. Nevertheless, a very good approximation of the Mw increase is obtained assuming that only one molecule of DPPC is transferred from the micelles to the enzyme active site pocket. With the DPPC-NaTDC mixed micelles, 1 molecule of DPPC would be transferred with 8 molecules of NaTDC (+4908 Da vs. 4964 Da estimated by SEC; Table 2). While with the DPPC-NaGDC mixed micelles, 1 molecule of DPPC would be transferred with 7 molecules of NaGDC (+4035 Da vs. 4040 Da estimated by SEC; Table 2).

The lyso-C16-PC-NaTDC dispersion was the third type of bile salt-containing micelles for which the phospholipid substrate was efficiently hydrolyzed by GPLRP2 (Fig. 1). Bile salts are therefore required for the hydrolysis of both DPPC and lyso-C16-PC, but in this later case, the hydrolysis seems to be mediated by the short-life interaction with smaller micelles (Table 1) that are not visible by SEC and GPLRP2 association with a limited number of surfactant molecules. There is here some contradiction between the SEC data giving a hydrodynamic diameter of 5.8 nm for the lyso-C16-PC-NaTDC mixed micelles with GPLRP2 S152G and the DLS data showing an increase in the hydrodynamic diameter from 3.4 nm with the pure micelles to 64.6 nm in the presence of GPLRP2 S152G (Table 1). This later value is however the z-average value of a mixture of 3 apparent populations centered at 4, 35 and 1500 nm as seen in Fig. 2.

4.3. Differences between DPPC-bile salt and DPPC- triton X-100 mixed micelles

In general, the perturbations of DPPC acyl chain fluidity and thermotropic properties were higher in mixed micelles containing NaGDC and NaTDC than in micelles made with Triton X-100 and DPPC LUV (Figs. 4 and 5 and Table 3). The similar effects of NaTDC and NaGDC are not surprising since they are both dihydroxy bile salts and they possess similar hydrophobic/hydrophilic balance with a log P of 5.79 and 4.45 respectively. Other non-conjugated dihydroxy bile salts, such as sodium deoxycholate (NaDC), are known to perturb lipid acyl chains fluidity and phase transition in a similar manner (Chantres et al., 1996). Similar observations have also been made with systems containing phospholipid and other sterols derivatives such as cholesterol (Umemura et al., 1980), suggesting that sterol-related molecules might have the same general effect on phospholipid acyl chains. Because they are related to cholesterol, bile salts such as NaTDC and NaGDC are not classical head-to-tail amphiphiles. Indeed, they present a concave molecular geometry with a hydrophobic surface on one side and a hydrophilic surface on the other side where hydroxyl groups are found (Hofmann, 2009; Small et al., 1969). On the other hand, Triton X-100 shows a clear-cut separation between its hydrophobic 4-octylphenol group and its hydrophilic poly-ethoxylene group (Robson and Dennis, 1977, 1978). These particularities in the respective distributions of polar and apolar regions in Triton X-100 and bile salts result in different interactions of theses surfactants with DPPC molecules and they may account for many of the spectral differences observed in the mid-IR region.

The interfacial region of water-dispersed phospholipid aggregates is constantly interacting with water and solute molecules resulting in hydration and/or H-bonding of the carbonyl groups. Changes in hydration and H-bonding affect the energy of the CO bond and thus its IR spectral stretching vibration frequency (Hubner and Blume, 1998; Pohle et al., 1998). We observed that NaGDC and Triton X-100 affected differently the hydration and H-bonding of the CO group of DPPC molecules in mixed micelles. As previously observed with NaTDC (Mateos-Diaz et al., 2017b), NaGDC is increasing the interfacial hydration while Triton X-100 is decreasing it (Fig. 6 and Table 3). A bile salt-induced increase in the interfacial hydration of phospholipids has been previously observed by fluorescence experiments using DPPC and DMPC bilayers and bile salts at sub-micellar concentrations (Mohapatra and Mishra, 2011). Triton X-100 seems to be accommodated more orderly between DPPC molecules and its large hydrophilic poly-(oxyethylene)-chain (17 Å) may affect the topology of the interface and

dehydrate the interfacial CO groups of DPPC molecules as suggested by the lower CO subcomponents intensity ratios observed for this system (Table 3). It worth mentioning that these values are even lower than those observed with DPPC liposomes (Mateos-Diaz et al., 2017b), suggesting a more anhydrous and less “penetrable” interface. This could result from the possible sequestration of a high number of water molecules by the poly-(oxyethylene)-chain of TX100 molecules (Kamenka et al., 1991; Nilsson and Lindman, 1983). However, another important factor that should be taken into account is the interfacial charge, which evidently differs between anionic bile salts and non-ionic Triton X-100 and that certainly play an important role in the interfacial polarity, hydration and H-bonding.

The IR spectrum regions assigned to polar head group, containing mainly phosphate (PO)-related vibrations, are also affected by hydration and H-bonding with the solvent and solutes. As previously observed with DPPC-NaTDC mixed micelles (Mateos-Diaz et al., 2017b), the PO group in DPPC-NaGDC dispersions is slightly more hydrated than in DPPC liposomes, but also than in DPPC-TX100 mixed micelles (Fig. 7 and Table 3). Interestingly, the IR spectrum of DPPC-NaGDC but not DPPC-TX100 mixed micelles displays a lower energy vibration band (1050 cm^{-1}) that might be associated with the head-group conformation. Previous studies have shown that Triton X-100 can decrease the hydration of DPPC phosphate group and also the intensity of the R-O-P-O-R’ vibration (Goni and Arrondo, 1986; Goni et al., 1986), which is in agreement with our findings.

4.4. GPLRP2 S152G interacts preferentially with mixed micelles containing bile salts

The addition of GPLRP2 S152G variant to mixed micelle solutions results in relatively important changes in spectral parameters for the DPPC-NaGDC mixed micelles, but not for the DPPC-Triton X-100 system, indicating that GPLRP2 interacts preferentially with mixed micelles containing anionic bile salts instead of non-ionic Triton X-100. Apart from the surface charge that could favor GPLRP2 interaction, IR spectroscopy analysis suggests how the packing/fluidity of DPPC acyl chains and interfacial hydration/H-bonding could favor the interaction of GPLRP2 with DPPC-bile salt mixed micelles.

GPLRP2 S152G variant slightly increases the T_m of both DPPC-NaGDC and DPPC-NaTDC dispersions (Table S1 and Fig. 5) and decreases the acyl chain fluidity (Fig. 4 and Table 3), thus reversing the effects induced by bile salts upon formation of mixed micelles from pure DPPC vesicles (Mateos-Diaz et al., 2017b). These effects might be caused by the partial insertion of GPLRP2 hydrophobic loops into DPPC-bile salt micelle interface upon formation of enzyme-micelle complexes. They are however opposed to what has been observed with integral membrane proteins, which strongly increase the hydrophobic acyl chains mobility in lipid bilayers and at very high protein-to-lipid ratio, completely abolish the main phase transition (Arrondo and Goñi, 1998; Cortijo et al., 1982; Cortijo and Chapman, 1981; Lee and Chapman, 1986; Mendelsohn et al., 1981). The interactions of peripheral membrane proteins with lipid membranes are known to be more diverse and they can affect IR vibrations at various molecular levels (*i.e.* hydrophobic acyl chains, interfacial CO and polar head-group) (Arrondo and Goñi, 1998; Nabet et al., 1994). However, when peripheral membrane proteins are able to affect the hydrophobic moieties of lipid bilayers, their effects are similar to those observed with integral membrane protein but they are less intense (Nabet et al., 1994). Therefore, GPLRP2 also differs from peripheral membrane proteins. It is worth recalling here that GPLRP2 only hydrolyzes phospholipid monolayers at low surface pressure, with a maximum activity on phosphatidylcholine at 5 mN/m (Hjorth et al., 1993). This means that GPLRP2 is not a highly penetrating enzyme compared to other phospholipases like PLA2 from snake venoms (Boffa et al., 1980; Verheij et al., 1980). Experiments with DPPC-TX100 mixed micelles and liposomes confirm that GPLRP2 does not establish lipid-protein interaction nor display a hydrolytic activity on systems with a rigid hydrophobic core. It prefers substrates with more fluid hydrophobic acyl chains like DPPC-bile salt micelles or monolayers at low surface pressure, probably because it favors the penetration of the hydrophobic surface loops of GPLRP2 (Dridi et al., 2013) inside the lipid particle and the subsequent recruitment of a phospholipid molecule in the active site (Fig. 8). This mechanism is supported by the rigidification of the acyl chains when the GPLRP2 S152G variant interacts with DPPC-bile salt micelles.

The dehydration of the interfacial CO groups upon addition of GPLRP2 S152G variant is only observed with DPPC dispersions containing bile salts (Fig. 6, Table 3 and Fig. S3). As previously proposed (Mateos-Diaz et al., 2017b), one possible explanation is the expulsion of water molecules from the interface when the enzyme-micelle complex is formed and hydrophobic interactions established between the GPLRP2 hydrophobic loops and DPPC acyl chains (Fig. 8). The protein may also simply act as an amphiphile altering the interfacial distribution of DPPC and bile salts, and thus reducing the effects of bile salts which promotes interfacial H-bonding with the solvent. This effect of GPLRP2 would be opposed to what is observed with integral membrane proteins which induce a higher hydration of the CO group of phospholipids in bilayers (Bhushan and McNamee, 1990), and therefore act more like bile salts. Indeed, it seems that GPLRP2 S152G tends to interact with substrates displaying a higher interfacial hydration and H-bonding, such as bile salt-containing mixed micelles, rather than with more anhydrous and less H-bonded systems like liposomes and DPPC-TX100 mixed micelles.

4.5. Bile salts enhance the lipolytic activity of GPLRP2 on lysophospholipid by inducing slight changes in the interfacial properties of micelles

Lysophospholipids are products of the lipolysis reaction catalyzed by phospholipases and they can also be substrates for some of these enzymes. GPLRP2 for instance shows a main PLA1 activity and can act on both di-acyl-glycero-phospholipids and *sn*-1-mono-acyl-glycero-phospholipids. It is therefore worth studying GPLRP2 interaction with lysophospholipids as we did it with DPPC. Lyso-C16-PC was selected because it could be generated from DPPC. Its dispersions in water are organized in small micelles (7 nm) with a constant size at temperatures ranging from 25 to 70 °C (Fig. S1). The hydrophobic acyl chains of lyso-C16-PC micelles are highly disordered and show a higher mobility compared to acyl chains in DPPC micelles, as indicated by the highest CH2 stretching vibration frequency and FWHM values recorded among all the tested lipid dispersions (Fig. 4, Table 3 and Fig. S2). Addition of GPLRP2 S152G variant does affect the order/disorder proportion, but it increases the mobility of the acyl chains when NaTDC is also present. This might be related to the formation of larger particles (Fig. 2) that could favor GPLRP2-micelle interactions. Interestingly, GPLRP2 is only active on lyso-C16-PC-bile salt mixed micelles as observed with DPPC (Fig. 1).

The interfacial CO group of lyso-C16-PC is characterized by a wider and more complex stretching vibration band, and it appears to be in a more hydrated environment compared to CO groups in DPPC dispersions (Fig. 6). After deconvolution, the CO-spectra of lyso-C16-PC-containing micelles appears very similar to those observed with alkyl-acyl-phosphatidylcholines with three subcomponents instead of the two classically observed with DPPC dispersions (Lewis et al., 1994). Other studies also highlight the higher degree of H-bonding of CO-groups in lyso-PC molecules (Frias et al., 2008). The line shape of CO band is changed in the presence of NaTDC, which might reflect a reduced mobility of CO groups and a decrease in the corresponding subcomponent width. GPLRP2 S152G variant does not exert any effect on lyso-C16-PC CO group but, interestingly, it induces NaTDC-dependent changes at the polar head-group region, while no changes are observed in the presence of NaTDC without the protein (Fig. 7). Vibrations in this region have been previously assigned to the R—O—P—O—R’ group (Arrondo et al., 1984), but it is also reported that some contribution of

C—O—C vibrations might be present (Fringeli and Gunthard, 1981; Goni and Arrondo, 1986; Mendelsohn and Mantsch, 1985). In any case, it seems that changes in H-bonding/hydration and mobility of CO group caused by NaTDC at the interfacial CO-group might be related with the capacity of GPLRP2 S152G variant to interact and thus affect the headgroup vibrations. This would be a different way of interaction, which would also explain the lower activity of GPLRP2 on lyso-C16-PC compared to DPPC. Alternatively, NaTDC molecules may preferentially interact with GPLRP2 S152G variant and indirectly change the enzyme-lyso-C16-PC interaction. In experiments with DPPC-bile salt micelles we have shown that GPLRP2 S152G variant could be associated with a few monomers of bile salts and/or DPPC and form low Mw aggregates, probably after a first encounter with high Mw mixed micelles. In the context of the whole lipolysis reaction, the hydrolysis of lysophospholipids is therefore likely to occur after their interaction with bile salt-associated GPLRP2.

5. Conclusion

The observations made with phospholipid-bile salt micelles suggest that the hydrolysis of phospholipid molecules by GPLRP2 can be mediated by the transient formation of “large” one-to-one enzyme-micelle complexes, leading to the extraction of one DPPC molecule from the micelle and followed by the dissociation of the enzyme still associated with bile salt monomers (Fig. 8). This hypothesis is well supported by the numerous observations made by X-ray crystallography of surfactant monomers bound to the hydrophobic side of lipases (Delorme et al., 2011; Mateos-Diaz et al., 2017a). It is also well known that when lipases have been in contact with surfactants, large molecular weight aggregates can be observed (as seen here with Triton X100) and some monomers always remain bound to the enzyme (Mateos-Diaz et al., 2007). The mechanism proposed here for GPLRP2 acting on micelles is reminiscent of the mechanism proposed by Scott et al. for sPLA2, with the phospholipid transfer from the membrane to the protein occurring at the interface (Scott et al., 1990), but there is no evidence that the hydrolysis reaction also takes place at the micelle interface. The catalysis of ester bond cleavage might also take place in the soluble phase after dissociation of low Mw GPLRP2 aggregates. After conversion of the substrate, the hydrolysis products, bile salts and the enzyme may be re-associated with larger mixed micelles to ensure the catalytic cycle and complete phospholipid digestion. GPLRP2 could thus undergo a fast exchange between micelles and act according to the so-called “hopping mode” (Jain and Berg, 1989), a mechanism also observed with classical pancreatic lipase acting on lipid droplets (Haiker et al., 2004).

We highlight here the importance of bile salts for phospholipid digestion. They can change the properties of lipid/water interfaces (acyl chain fluidity, hydration and H-bonding), facilitate enzyme-micelle interaction and thus promote an efficient mass transfer between micelles and enzyme during the lipolysis reaction. These specific features are not observed with the non-ionic surfactant Triton X-100.

Contributions

Dr Eduardo Mateos-Diaz was involved in the conception and design of the study, in acquisition, analysis and interpretation of data on protein production, IR spectroscopy, SEC, DLS and enzyme assays, in drafting the article and revising it critically for important intellectual content. Dr Priscila Sutto-Ortiz was involved in the acquisition, analysis and interpretation of data related to phospholipid hydrolysis and size exclusion chromatography. Moulay Sahaka, MSc, was involved in the acquisition, analysis and interpretation of data related to IR spectroscopy. Dr Deborah Byrne was involved in the acquisition, analysis and interpretation of data related to DLS. Dr Hélène Gaussier was involved in the conception and design of the study, in analysis and interpretation of IR data. Dr Frédéric Carrière was involved in the conception and design of the study, in drafting the article, revising it critically for important intellectual content and final approval of the version to be submitted. All authors were involved in the final approval of the version to be submitted.

Conflict of interest

All authors declare no conflict of interest.

Acknowledgements

Eduardo Mateos-Diaz and Priscila Sutto-Ortiz are grateful to CONACYT for the financial support received during their PhD thesis (scholarship ID 217854/313389 for E.M.D. and 376598/247081 for P.S.O). Moulay Sahaka is grateful to Aix Marseille Université for his PhD scholarship. This work was supported by Centre National de la Recherche Scientifique.

References

Almgren, M., 2000. Mixed micelles and other structures in the solubilization of bilayer lipid membranes by surfactants. Biochim. Biophys. Acta (BBA) – Biomembr. 1508, 146–163.

Arrondo, J.L.R., Goñi, F.M., 1998. Infrared studies of protein-induced perturbation of lipids in lipoproteins and membranes. Chem. Phys. Lipids 96, 53–68.

Arrondo, J.L.R., Goñi, F.M., Macarulla, J.M., 1984. Infrared-spectroscopy of phosphatidylcholines in aqueous suspension – a study of the phosphate group vibrations. Biochim. Biophys. Acta 794, 165–168.

Berg, O.G., Yu, B.Z., Rogers, J., Jain, M.K., 1991. Interfacial catalysis by phospholipase A2: determination of the interfacial kinetic rate constants. Biochemistry 30, 7283–7297.

Berg, O.G., Gelb, M.H., Tsai, M.D., Jain, M.K., 2001. Interfacial enzymology: the secreted phospholipase A(2)-paradigm. Chem. Rev. 101, 2613–2654.

Bhushan, A., McNamee, M.G., 1990. Differential scanning calorimetry and Fourier transform infrared analysis of lipid protein interactions involving the nicotinic acetylcholine receptor. Biochim. Biophys. Acta 1027, 93–101.

Boffa, M.-C., Rothen, C., Verheij, H.M., Verger, R., de Haas, G.H., 1980. Classification of phospholipases A2 based upon their anticoagulant activity and penetration ability into phospholipid monolayers. In: Eaker, D., Wadström, T. (Eds.), Natural Toxins. Pergamon Press, OxFord and New York, pp. 131–138.

Chantres, J.R., Elorza, B., Elorza, M.A., Rodado, P., 1996. Deoxycholate alters the order of acyl chains in freeze-thaw extrusion vesicles of L-alpha-dipalmitoyl phosphatidylcholine: study of the 1,6-diphenyl-1,3,5-hexatriene steady-state fluorescence anisotropy. Int. J. Pharm. 138, 139–148.

Cohen, D.E., Thurston, G.M., Chamberlin, R.A., Benedek, G.B., Carey, M.C., 1998. Laser light scattering evidence for a common wormlike growth structure of mixed micelles in bile salt- and straight-chain detergent-phosphatidylcholine aqueous systems: relevance to the micellar structure of bile. Biochemistry 37, 14798–14814.

Cortijo, M., Chapman, D., 1981. A comparison of the interactions of cholesterol and gramicidin A with lipid bilayers using an infrared data station. FEBS Lett. 131, 245–248.

Cortijo, M., Alonso, A., Gomez-Fernandez, J.C., Chapman, D., 1982. Intrinsic protein-lipid interactions – infrared spectroscopic studies of gramicidin-A, bacteriorhodopsin and Ca-2+-ATPase in biomembranes and reconstituted systems. J. Mol. Biol. 157, 597–618.

De Caro, J., Carrière, F., Barboni, P., Giller, T., Verger, R., de Caro, A., 1998. Pancreatic lipase-related protein 1 (PLRP1) is present in the pancreatic juice of several species. Biochim. Biophys. Acta 1387, 331–341.

De Haas, G.H., Postema, N.M., Nieuwenhuizen, W., van Deenen, L.L., 1968. Purification and properties of phospholipase A from porcine pancreas. Biochim. Biophys. Acta 159, 103–117.

Deems, R.A., Eaton, B.R., Dennis, E.A., 1975. Kinetic analysis of phospholipase A2 activity toward mixed micelles and its implications for the study of lipolytic enzymes. J. Biol. Chem. 250, 9013–9020.

Delorme, V., Dhouib, R., Canaan, S., Fotiadu, F., Carriere, F., Cavalier, J.F., 2011. Effects of surfactants on lipase structure, activity, and inhibition. Pharm. Res. 28, 1831–1842.

Dennis, E.A., 1973. Kinetic dependence of phospholipase A 2 activity on the detergent Triton X-100. J. Lipid Res. 14, 152–159.

Dennis, E.A., 1974. Formation and characterization of mixed micelles of the nonionic surfactant Triton X-100 with egg, dipalmitoyl, and dimyristoyl phosphatidylcholines. Arch. Biochem. Biophys. 165, 764–773.

Dridi, K., Amara, S., Bezzine, S., Rodriguez, J.A., Carriere, F., Gaussier, H., 2013. Partial deletion of beta9 loop in pancreatic lipase-related protein 2 reduces enzyme activity with a larger effect on long acyl chain substrates. Biochim. Biophys. Acta 1831, 1293–1301.

Egelhaaf, S.U., Schurtenberger, P., 1999. Micelle-to-vesicle transition: a time-resolved structural study. Phys. Rev. Lett. 82, 2804–2807.

Frias, M.A., Winik, B., Franzoni, A.B., Levstein, P.R., Nicastro, A., Gennaro, A.A., Diaz, S.B., Disalvo, E.A., 2008. Lysophosphatidylcholine-arbutin complexes form bilayer-

like structures. Biochim. Biophys. Acta–Biomembr. 1778, 1259–1266.
Fringeli, U.P., Gunthard, H.H., 1981. Infrared membrane spectroscopy. Mol. Biol. Biochem. Biophys. 31, 270–332.
Gagos, M., Koper, R., Gruszecki, W.I., 2001. Spectrophotometric analysis of organisation of dipalmitoylphosphatidylcholine bilayers containing the polyene antibiotic amphotericin B. Biochim. Biophys. Acta–Biomembr. 1511, 90–98.
Gelb, M.H., Jain, M.K., Hanel, A.M., Berg, O.G., 1995. Interfacial enzymology of glycerolipid hydrolases: lessons from secreted phospholipases A2. Annu. Rev. Biochem 64, 653–688.
Goni, F.M., Arrondo, J.L.R., 1986. A study of phospholipid phosphate groups in model membranes by Fourier-transform infrared-spectroscopy. Faraday Discuss. 81, 117–126.
Goni, F.M., Urbaneja, M.A., Arrondo, J.L.R., Alonso, A., Durrani, A.A., Chapman, D., 1986. The interaction of phosphatidylcholine bilayers with Triton X-100. Eur. J. Biochem. 160, 659–665.
Haiker, H., Lengsfeld, H., Hadvary, P., Carrière, F., 2004. Rapid exchange of pancreatic lipase between triacylglycerol droplets. Biochim. Biophys. Acta 1682, 72–79.
Helenius, A., Simons, K., 1975. Solubilization of membranes by detergents. Biochim. Biophys. Acta 415, 29–79.
Hermoso, J., Pignol, D., Kerfelec, B., Crenon, I., Chapus, C., Fontecilla-Camps, J.C., 1996. Lipase activation by nonionic detergents. The crystal structure of the porcine lipase-colipase-tetraethylene glycol monooctyl ether complex. J. Biol. Chem. 271, 18007–18016.
Hernell, O., Olivecrona, T., 1974. Human milk lipases: II. Bile salt stimulated lipase. Biochim. Biophys. Acta 369, 234–244.
Hjelm, R.P., Thiyagarajan, P., Alkan-Onyuksel, H., 1992. Organization of phosphatidylcholine and bile salt in rodlike mixed micelles. J. Phys. Chem. 96, 8653–8661.
Hjorth, A., Carrière, F., Cudrey, C., Wöldike, H., Boel, E., Lawson, D.M., Ferrato, F., Cambillau, C., Dodson, G.G., Thim, L., Verger, R., 1993. A structural domain (the lid) found in pancreatic lipases is absent in the guinea pig (phospho)lipase. Biochemistry 32, 4702–4707.
Hofmann, A.F., 2009. Bile acids: trying to understand their chemistry and biology with the hope of helping patients. Hepatology 49, 1403–1418.
Hubner, W., Blume, A., 1998. Interactions at the lipid-water interface. Chem. Phys. Lipids 96, 99–123.
Jain, M.K., Berg, O.G., 1989. The kinetics of interfacial catalysis by phospholipase A2 and regulation of interfacial activation: hopping versus scooting. Biochim. Biophys. Acta 1002, 127–156.
Jain, M.K., Gelb, M.H., Rogers, J., Berg, O.G., 1995. Kinetic basis for interfacial catalysis by phospholipase A2. Methods Enzymol. 249, 567–614.
Kamenka, N., El Amrani, M., Appell, J., Lindheimer, M., 1991. Mixed micelle-to-vesicle transition in aqueous nonionic phospholipid systems. J. Colloid Interface Sci. 143, 463–471.
Kirchhoff, W.H., Levin, I.W., 1987. Description of the thermotropic behavior of membrane bilayers in terms of RAMAN spectral parameters – a 2-state model. J. Res. Nat. Bur. Stand. 92, 113–128.
Kozlov, M.M., Lichtenberg, D., Andelman, D., 1997. Shape of phospholipid/surfactant mixed micelles: cylinders or disks? Theoretical analysis. J. Phys. Chem. B 101, 6600–6606.
Lee, D.C., Chapman, D., 1986. Infrared spectroscopic studies of biomembranes and model membranes. Biosci. Rep. 6, 235–256.
Lewis, R., McElhaney, R.N., Pohle, W., Mantsch, H.H., 1994. Components of the carbonyl stretching band in the infrared-spectra of hydrated 1,2-diacylglycerolipid bilayers – a reevaluation. Biophys. J . 67, 2367–2375.
Madenci, D., Salonen, A., Schurtenberger, P., Pedersen, J.S., Egelhaaf, S.U., 2011. Simple model for the growth behaviour of mixed lecithin-bile salt micelles. Phys. Chem. Chem. Phys. 13, 3171–3178.
Mateos-Diaz, J.C., Cordova, J., Baratti, J., Carriere, F., Abousalham, A., 2007. Effect of nonionic surfacants on Rhizopus homothallicus lipase activity – a comparative kinetic study. Mol. Biotechnol. 35, 205–214.
Mateos-Diaz, E., Amara, S., Roussel, A., Longhi, S., Cambillau, C., Carriere, F., 2017a. Probing conformational changes and interfacial recognition site of lipases with surfactants and inhibitors. Methods Enzymol. 583, 279–307.
Mateos-Diaz, E., Bakala N'Goma, J.C., Byrne, D., Robert, S., Carriere, F., Gaussier, H., 2017b. IR spectroscopy analysis of pancreatic lipase-related protein 2 interaction with phospholipids: 1. Discriminative recognition of mixed micelles versus liposomes. Chem. Phys. Lipids.
Mazer, N.A., Benedek, G.B., Carey, M.C., 1980. Quasielastic light-scattering studies of aqueous biliary lipid systems: mixed micelle formation in bile salt-lecithin solutions. Biochemistry 19, 601–615.
Mendelsohn, R., Mantsch, H.H., 1985. Fourier transform infrared studies of lipid-protein interactions. In: Watts, A., Pont, J.J.H.H.M.D. (Eds.), Progress in Protein-Lipid Interactions. Elsevier, Amsterdam, pp. 1103–1146.
Mendelsohn, R., Dluhy, R., Taraschi, T., Cameron, D.G., Mantsch, H.H., 1981. RAMAN and Fourier-transform infrared spectroscopic studies of the interaction between glycophorin and dimyristoylphosphatidylcholine. Biochemistry 20, 6699–6706.
Mohapatra, M., Mishra, A.K., 2011. Effect of submicellar concentrations of conjugated and unconjugated bile salts on the lipid bilayer membrane. Langmuir 27, 13461–13467.
Nabet, A., Boggs, J.M., Pezolet, M., 1994. Study by infrared-spectroscopy of the interaction of bovine myelin basic-protein with phosphatidic-acid. Biochemistry 33, 14792–14799.
Nichols, J.W., Ozarowski, J., 1990. Sizing of lecithin-bile salt mixed micelles by size-exclusion high-performance liquid-chromatography. Biochemistry 29, 4600–4606.
Nilsson, P.G., Lindman, B., 1983. Water self-diffusion in nonionic surfactant solutions: hydration and obstruction effects. J. Phys. Chem. 87, 4756–4761.
Panaitov, I., Ivanova, M., Verger, R., 1997. Interfacial and temporal organization of enzymatic lipolysis. Curr. Opin. Colloid Interface Sci. 2, 517–525.
Pohle, W., Selle, C., Fritzsche, H., Binder, H., 1998. Fourier transform infrared spectroscopy as a probe for the study of the hydration of lipid self-assemblies: I. I. Methodology and general phenomena. Biospectroscopy 4, 267–280.
Robson, R.J., Dennis, E.A., 1977. Size, shape, and hydration of nonionic surfactant micelles – Triton X-100. J. Phys. Chem. 81, 1075–1078.
Robson, R.J., Dennis, E.A., 1978. Characterization of mixed micelles of phospholipids of various classes and a synthetic, homogeneous analog of non-ionic detergent Triton X-100 containing 9 oxyethylene groups. Biochim. Biophys. Acta 508, 513–524.
Schurtenberger, P., Mazer, N., Kanzig, W., 1985. Micelle to vesicle transition in aqueous-solutions of bile-salt and lecithin. J. Phys. Chem. 89, 1042–1049.
Scott, D.L., White, S.P., Otwinowski, Z., Yuan, W., Gelb, M.H., Sigler, P.B., 1990. Interfacial catalysis: the mechanism of phospholipase A2. Science 250, 1541–1546.
Small, D.M., Penkett, S.A., Chapman, D., 1969. Studies on simple and mixed bile salt micelles by nuclear magnetic resonance spectroscopy. Biochim. Biophys. Acta 176, 178–189.
Umemura, J., Cameron, D.G., Mantsch, H.H., 1980. A Fourier-transform infrared spectroscopic study of the molecular interaction of cholesterol with 1,2-dipalmitoyl-sn-glycero-3-phosphocholine. Biochim. Biophys. Acta 602, 32–44.
Uversky, V.N., 1993. Use of fast protein size-exclusion liquid-chromatography to study the unfolding of proteins which denature through the molten globule. Biochemistry 32, 13288–13298.
Verger, R., De Haas, G.H., 1973. Enzyme reactions in a membrane model. 1. A new technique to study enzyme reactions in monolayers. Chem. Phys. Lipids 10, 127–136.
Verger, R., Mieras, M.C., de Haas, G.H., 1973a. Action of phospholipase A at interfaces. J. Biol. Chem. 248, 4023–4034.
Verger, R., Mieras, M.C.E., de Haas, G.H., 1973b. Action of phospholipase A2 at interfaces. J. Biol. Chem. 248, 4023–4034.
Verheij, H.M., Boffa, M.C., Rothen, C., Bryckaert, M.C., Verger, R., de Haas, G.H., 1980. Correlation of enzymatic activity and anticoagulant properties of phospholipase A2. Eur. J. Biochem. 112, 25–32.
Walter, A., Vinson, P.K., Kaplun, A., Talmon, Y., 1991. Intermediate structures in the cholate-phosphatidylcholine vesicle-micelle transition. Biophys. J . 60, 1315–1325.
Withers-Martinez, C., Carriere, F., Verger, R., Bourgeois, D., Cambillau, C., 1996. A pancreatic lipase with a phospholipase A1 activity: crystal structure of a chimeric pancreatic lipase-related protein 2 from guinea pig. Structure 4, 1363–1374.
de Haas, G.H., Postema, N.M., Nieuwenhuisen, W., L.L.M.v.D, 1971. Studies on phospholipase A and its zymogen from porcine pancreas. III. Action of the enzyme on short-chain lecithins. Biochim. Biophys. Acta 239, 252–266.